A coherently stimulated Brillouin spectrometer

Joel N. Johnson,[1,2,*] Peter T. Rakich,[3] Co Authors,[4] and Ryan O. Behunin[1,2,†]

[1] *Department of Applied Physics and Materials Science, Northern Arizona University, Flagstaff, AZ, 86011, USA*
[2] *Center for Materials Interfaces in Research and Applications, Northern Arizona University, Flagstaff, AZ, 86011, USA*
[3] *Department of Applied Physics, Yale University, New Haven, CT, 06520, USA*
[4] *Department, Address*

(Dated: May 10, 2024)

ALorem ipsum dolor sit amet, consectetur adipiscing elit. Nulla eget dolor at diam volutpat congue sit amet non magna. Phasellus sed ante ornare, commodo elit id, euismod enim. Mauris posuere, erat id vehicula ultrices, erat nisi faucibus lorem, at vehicula enim orci in dui. Nulla facilisi. Integer sed tortor venenatis, aliquet nulla quis, fermentum libero. Proin sit amet metus nec ante fermentum gravida at nec odio. Praesent id nisi ut sapien rutrum hendrerit. Donec vel sapien et eros accumsan tempus. Maecenas non velit nec nulla cursus faucibus sit amet sed dui. Ut eleifend, magna in fermentum efficitur, ligula ipsum blandit libero, sed iaculis eros magna ut arcu. Fusce eget lectus aliquet, consequat dolor at, aliquam urna. Curabitur pharetra, arcu sed vehicula maximus, nibh leo sollicitudin elit, vitae dapibus odio metus gravida ante. Aliquam erat volutpat. Donec venenatis erat vel ultrices suscipit. Nulla consequat massa quis enim. Donec pede justo, fringilla vel, aliquet nec, vulputate eget, arcu. In enim justo, rhoncus ut, imperdiet a, venenatis vitae, justo.

I. INTRODUCTION

Brillouin scattering is the inelastic scattering of light from acoustic phonons. Spontaneous Brillouin scattering is light scattering specifically with the thermodynamic fluctuations in a material. Sufficient optical power elevates this spontaneous process into stimulated Brillouin scattering: a regime in which the optical fields augment the optical properties of the material, greatly enhancing the optomechanical response. This occurs as the backscattered (e.g. Stokes) light beats with the incident pump light to induce an electrostrictive modulation that reinforces the acoustic phonons in the material. It would be desirable to introduce a high-powered fourth optical field dedicated to electrostrictive reinforcement, further stimulating the acoustic field, however phase matching conditions require that its frequency and wavevector be identical to that of the backscattered light, preventing distinguishability.

In this work, we present a coherently stimulated Brillouin spectrometer that utilizes a detuned pump-probe design to perform traveling-wave phonon spectroscopy at scales previously unachievable with traditional stimulated Brillouin techniques. With this method, we achieve sub-10 femtowatt sensitivity and enable room temperature traveling-wave phonon spectroscopy at the micrometer scale. We demonstrate the capabilities of the instrument by observing Brillouin scattering at room temperature in 1 centimeter of UHNA3 fiber and 100 micrometers of bulk carbon disulfide liquid. This instrument opens the door to nanometer-scale Brillouin spectroscopy with usage of higher optical powers and enables the characterization and development of novel nano-acousto-optic devices.

II. THEORETICAL FRAMEWORK

Coherently stimulated four-wave Brillouin scattering

Stimulated Brillouin scattering, illustrated by the schematic in Fig. **??**(a) for the Stokes process, is a three-wave mixing process in which incident pump laser light of frequency ω_{Pump} inelastically scatters from a traveling-wave phonon of frequency Ω to produce light that is frequency-shifted by the phonon frequency. In the Stokes process the phonon is retreating from the incident laser light and the scattered light is shifted down in frequency $\omega_{Stokes} = \omega_{Pump} - \Omega$. Light scattered in the backwards direction spatially overlaps with the incident laser light and thus the two optical fields interfere to produce a frequency at the difference between the two $\omega_{Pump} - \omega_{Stokes}$. Since this difference frequency is exactly equal to the frequency of the acoustic field Ω, the beating of the incident pump light and the backscattered Stokes light produces an electrostrictive reinforcement of the acoustic wave. This driving of the acoustic wave in turn increases the scattering rate of the incident pump light, producing a positive feedback process and an exponential increase of the amplitude of the backscattered Stokes wave.

Fig. **??**(b) shows the schematic of coherently stimulated four-wave Brillouin scattering for the Stokes process. We introduce a dedicated external Stokes laser of frequency ω_{Stokes} that strongly drives the electrostrictive reinforcement of the acoustic field in the material. The backscattered Stokes light which is normally collected in an SBS process to infer mechanical

* joel.johnson@nau.edu
† ryan.behunin@nau.edu

properties of the material is now drowned out by the much higher power external Stokes laser. To resolve this, we introduce an additional external laser at a distinct frequency ω_{Probe} which copropagates with the pump laser and backscatters in the material from the strongly driven acoustic field. This produces a backscattered signal to be collected, $\omega_{Signal} = \omega_{Probe} - \Omega$, which is distinguishable from the high-powered Stokes laser light. A full derivation of the coupled-wave equations for this four-wave mixing process can be found in Appendix B, where the scattered power of the backscattered signal is shown to be

$$P_{Sig} = (G_B L)^2 P_P P_S P_{Pr} sinc^2\left(\frac{\Delta k L}{2}\right), \qquad (1)$$

where G_B is the coherently stimulated Brillouin scattering gain factor,

$$G_B = g_0 \frac{\left(\frac{\Gamma_0}{2}\right)^2}{(\Omega - \Omega_B)^2 + \left(\frac{\Gamma_0}{2}\right)^2}, \qquad (2)$$

with the on-resonance gain factor of the material given by

$$g_0 = \left[\frac{\epsilon_0^2 \omega^2 q^4 \gamma_e^4}{4 n^2 c^2 \rho_0^2}\right]. \qquad (3)$$

Here, q is the wavevector of the driven acoustic field, γ_e is the electrostrictive constant, ρ_0 is the mean density of the material, Ω_B is the resonant Brillouin frequency of the material, Γ_B is the Brillouin linewidth, or dissipation rate, of the material, and Δk is the wavevector mismatch between the optical fields, to be discussed next.

Phase matching relaxation

In all nonlinear optical processes, efficiency is maximized when phase matching conditions are satisfied. A frequency mismatch (energy unconservation) or a wavevector mismatch (momentum unconservation) each result in drastically reduced efficiency of a given process.[1] This can be seen by Eq. 1, where the wavevector mismatch, Δk, is contained within a $sinc^2$ function. This $sinc^2$ term thereby defines the phase matching bandwidth of the system, notably scaling with effective interaction length L. For an effective length of one meter, a wavelength mismatch in UHNA3 fiber of only 0.6 pm drops the scattered power by half at 1.55um pump wavelength. However, for shorter effective lengths the permissible wavevector mismatch becomes more meaningful; a 36 pm wavelength separation preserves 82.5% of max signal for a length of 1 cm.

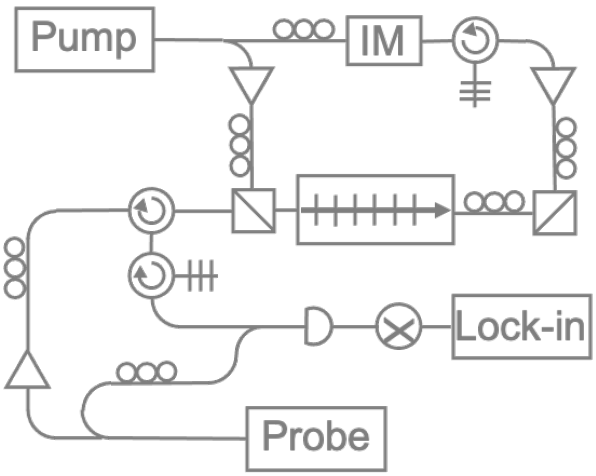

FIG. 1. CABS design diagram

III. METHODS

Instrument design

The design of the instrument is shown in the schematic in Fig. 1. A pump and Stokes signal is synthesized from a single tunable laser source for coherent stimulation of the sample. The pump signal (ω_{Pump}) is amplified by an erbium-doped fiber amplifier (EDFA) and passed through a variable optical attenuator (VOA) for power control. The output is then polarization-controlled to reflect at a polarizing beam splitter (PBS) for injection into the sample. For Stokes synthesis, an AC signal (Ω) is supplied to an intensity modulator with carrier frequency nulled and a tunable filter is used to select one side band output ($\omega_{Pump} - \Omega$). This Stokes light is then amplified by an EDFA, passed through a VOA, and polarization-controlled to reflect at a second PBS for couter-propagation to the pump through the sample.

A separate tunable laser ($\omega_{Probe} = \omega_{Pump} + \Delta k$) is used to synthesize the probe and local oscillator (LO). Probe light is amplified by an EDFA and fed through a VOA. A polarization controller aligns the polarization axis of the probe light for transmission through the first PBS and copropagation with the pump into the sample. Backscattered probe light exits the sample and transmits back through the first PBS, whereas the orthogonally polarized Stokes light reflects at this same point to be diverted to a tap for power monitoring. The backscattered signal ($\omega_{Signal} = \omega_{Probe} + \Omega$) then routes through two subsequent circulators for spectral filtering by a 5 GHz bandpass tunable filter. This filter allows the frequency-shifted probe light to pass while rejecting (1) any reflected probe light, and (2) any reflected, transmitted, or backscattered pump or Stokes light that was not already diverted by the PBS.

The filtered signal heterodynes via a 99-1 splitter with the LO ($\omega_{LO} = \omega_{Probe} + 2\pi \times 40MHz$), which has

been frequency-upshifted by an acousto-optic modulator (AOM) and controlled to be copolarized with the backscattered signal. We consider only the subtracted frequency term of the heterodyne process as all others (original, additive, higher-harmonic, and more complicated intermodulation product frequency terms) are well beyond the range of detection. This heterodyned signal ($\omega_{signal} = \Omega + 2\pi \times 40MHz$) is then captured by a photodiode detector and heterodyned again by a radio frequency (RF) mixer with a second AC signal ($\Omega - 2\pi \times 5MHz$) that synchronously sweeps with the Stokes-synthesis AC signal. The resulting constant signal ($\omega_{Lock-in} = 2\pi \times 45MHz$) is passed through a 50 MHz low-pass filter, amplified with an RF amplifier, and finally supplied to a lock-in amplifier for data collection. The lock-in amplifier is able to lock-in on the constant input frequency throughout a measurement as both AC signals, one supplied to the RF mixer and the other for Stokes synthesis, are synchronously swept through a range of frequencies during measurement.

IV. RESULTS

Measurements

We consider two example targets to demonstrate the capabilities of the instrument, one fiber-coupled and one bulk material. Fig. 2 shows the spectra captured for 1 cm of UHNA3 fiber. The spectral shape is that of the expected lorentzian function, with the peak ([9.18 GHz]) indicating the Brillouin resonance frequency and the FWHM ([80 MHz]) indicating the dissipation rate of the fiber. [comparison to regular SBS for some measurable length of UHNA3?]

Fig. shows the spectral measurements achieved by the instrument, overlaid with finite-difference simulation data. In Fig. we see the expected lorentzian spectral shape in good alignment with simulation data for guided longitudinal modes in the core of the UHNA3 fiber. In Fig. , however, we see a distortion of this lorentzian shape. This is expected for partially unguided longitudinal modes, such as is the case for a bulk liquid filling the volume of a ...

Fig. 2 shows a measurement of 1cm of UHNA3 fiber.

First, we measured Brillouin scattering in a 1-centimeter-long UHNA3 fiber at room temperature and with sub-Watt optical power (Fig.). Figure , clearly displays the Brillouin scattering features with remarkable signal-to-noise ratio, highlighting the effectiveness of our apparatus in isolating the backscattered probe light. This observation serves as one of the main showcases of the instrument's capability.

Next, we performed Brillouin scattering measurements on a 4-millimeter-thick bulk carbon disulfide sample in a free-space optics arrangement. The observed spectrum, presented in Figure 2, exhibits well-resolved Brillouin scattering peaks. This successful measurement in a bulk

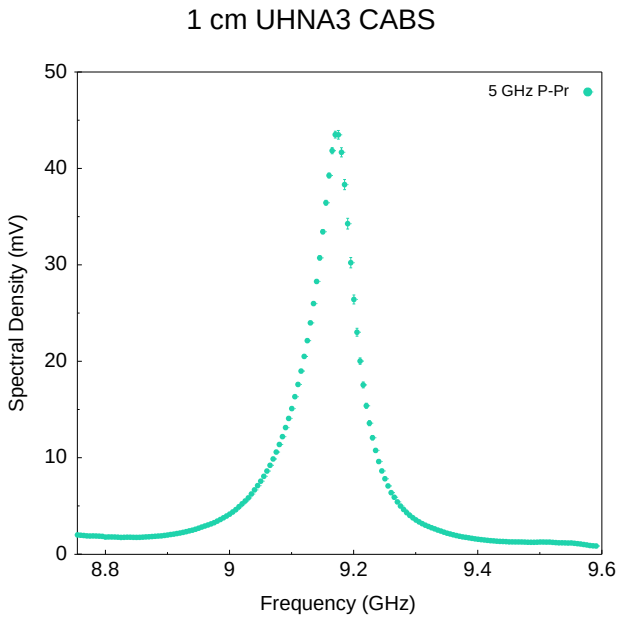

FIG. 2. 1cm UHNA3 (fit?)

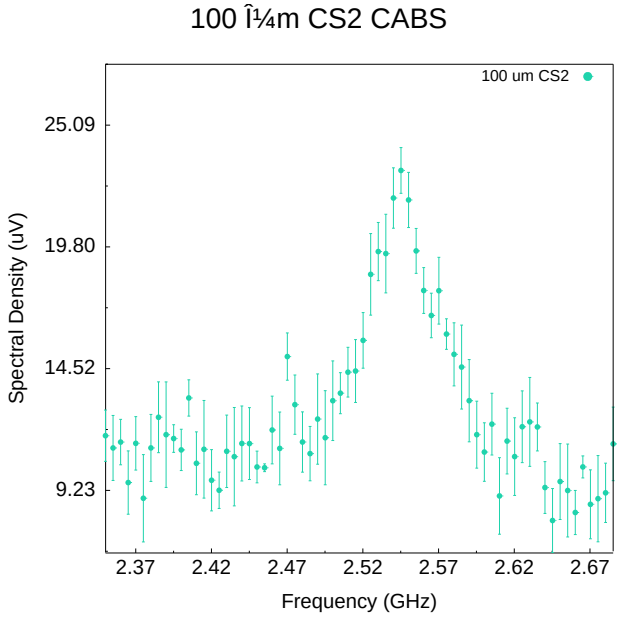

FIG. 3. 100um CS2

sample demonstrates the versatility and adaptability of our instrument to various experimental configurations, further emphasizing the instrument's capability.

Lastly, we conducted a measurement in a 1-millimeter-long UHNA3 fiber under low-power conditions, with only 10 microwatts of power at the sample. Despite the reduced sample length and low power, the instrument's sensitivity allowed us to observe distinct Brillouin scattering features in the spectrum, as illustrated in Figure 3. This result underscores the potential of our spectrometer for nanoscale measurements and serves as a demonstration of

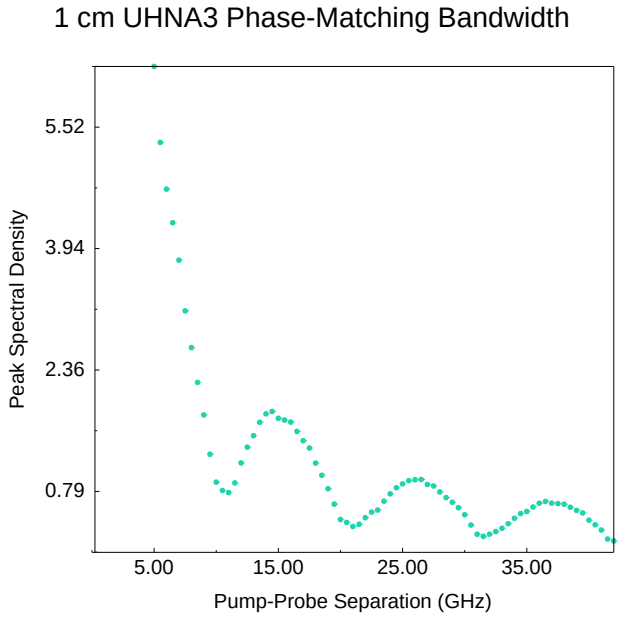

FIG. 4. Phase-matching sinc func

the instrument's sensitivity, defining the sensitivity floor of the apparatus.

These three observations collectively showcase the high sensitivity, broad applicability, and impressive capabilities of our coherent stimulated phonon spectrometer in measuring Brillouin scattering across different sample types, scales, and power levels.

Instrument sensitivity and SBS comparison

Lorem ipsum dolor sit amet, consectetuer adipiscing elit. Ut purus elit, vestibulum ut, placerat ac, adipiscing vitae, felis. Curabitur dictum gravida mauris. Nam arcu libero, nonummy eget, consectetuer id, vulputate a, magna. Donec vehicula augue eu neque. Pellentesque habitant morbi tristique senectus et netus et malesuada fames ac turpis egestas. Mauris ut leo. Cras viverra metus rhoncus sem. Nulla et lectus vestibulum urna fringilla ultrices. Phasellus eu tellus sit amet tortor gravida placerat. Integer sapien est, iaculis in, pretium quis, viverra ac, nunc. Praesent eget sem vel leo ultrices bibendum. Aenean faucibus. Morbi dolor nulla, malesuada eu, pulvinar at, mollis ac, nulla. Curabitur auctor semper nulla. Donec varius orci eget risus. Duis nibh mi, congue eu, accumsan eleifend, sagittis quis, diam. Duis eget orci sit amet orci dignissim rutrum.

Nam dui ligula, fringilla a, euismod sodales, sollicitudin vel, wisi. Morbi auctor lorem non justo. Nam lacus libero, pretium at, lobortis vitae, ultricies et, tellus. Donec aliquet, tortor sed accumsan bibendum, erat ligula aliquet magna, vitae ornare odio metus a mi. Morbi ac orci et nisl hendrerit mollis. Suspendisse ut massa. Cras nec ante. Pellentesque a nulla. Cum sociis natoque penatibus et magnis dis parturient montes, nascetur ridiculus mus. Aliquam tincidunt urna. Nulla ullamcorper vestibulum turpis. Pellentesque cursus luctus mauris.

Nulla malesuada porttitor diam. Donec felis erat, congue non, volutpat at, tincidunt tristique, libero. Vivamus viverra fermentum felis. Donec nonummy pellentesque ante. Phasellus adipiscing semper elit. Proin fermentum massa ac quam. Sed diam turpis, molestie vitae, placerat a, molestie nec, leo. Maecenas lacinia. Nam ipsum ligula, eleifend at, accumsan nec, suscipit a, ipsum. Morbi blandit ligula feugiat magna. Nunc eleifend consequat lorem. Sed lacinia nulla vitae enim. Pellentesque tincidunt purus vel magna. Integer non enim. Praesent euismod nunc eu purus. Donec bibendum quam in tellus. Nullam cursus pulvinar lectus. Donec et mi. Nam vulputate metus eu enim. Vestibulum pellentesque felis eu massa.

V. DISCUSSION

Lorem ipsum dolor sit amet, consectetuer adipiscing elit. Ut purus elit, vestibulum ut, placerat ac, adipiscing vitae, felis. Curabitur dictum gravida mauris. Nam arcu libero, nonummy eget, consectetuer id, vulputate a, magna. Donec vehicula augue eu neque. Pellentesque habitant morbi tristique senectus et netus et malesuada fames ac turpis egestas. Mauris ut leo. Cras viverra metus rhoncus sem. Nulla et lectus vestibulum urna fringilla ultrices. Phasellus eu tellus sit amet tortor gravida placerat. Integer sapien est, iaculis in, pretium quis, viverra ac, nunc. Praesent eget sem vel leo ultrices bibendum. Aenean faucibus. Morbi dolor nulla, malesuada eu, pulvinar at, mollis ac, nulla. Curabitur auctor semper nulla. Donec varius orci eget risus. Duis nibh mi, congue eu, accumsan eleifend, sagittis quis, diam. Duis eget orci sit amet orci dignissim rutrum.

Nam dui ligula, fringilla a, euismod sodales, sollicitudin vel, wisi. Morbi auctor lorem non justo. Nam lacus libero, pretium at, lobortis vitae, ultricies et, tellus. Donec aliquet, tortor sed accumsan bibendum, erat ligula aliquet magna, vitae ornare odio metus a mi. Morbi ac orci et nisl hendrerit mollis. Suspendisse ut massa. Cras nec ante. Pellentesque a nulla. Cum sociis natoque penatibus et magnis dis parturient montes, nascetur ridiculus mus. Aliquam tincidunt urna. Nulla ullamcorper vestibulum turpis. Pellentesque cursus luctus mauris.

VI. CONCLUSION

Lorem ipsum dolor sit amet, consectetuer adipiscing elit. Ut purus elit, vestibulum ut, placerat ac, adipiscing vitae, felis. Curabitur dictum gravida mauris. Nam arcu libero, nonummy eget, consectetuer id, vulputate a, magna. Donec vehicula augue eu neque. Pellentesque habitant morbi tristique senectus et netus et malesuada fames ac turpis egestas. Mauris ut leo. Cras viverra metus rhoncus sem. Nulla et lectus vestibulum urna fringilla

ultrices. Phasellus eu tellus sit amet tortor gravida placerat. Integer sapien est, iaculis in, pretium quis, viverra ac, nunc. Praesent eget sem vel leo ultrices bibendum. Aenean faucibus. Morbi dolor nulla, malesuada eu, pulvinar at, mollis ac, nulla. Curabitur auctor semper nulla. Donec varius orci eget risus. Duis nibh mi, congue eu, accumsan eleifend, sagittis quis, diam. Duis eget orci sit amet orci dignissim rutrum.

ACKNOWLEDGMENTS

Appendix:

A Coherently Stimulated Brillouin Spectrometer

Appendix A: Phase Matching

1. Relaxation of Phase Matching Conditions

2. Phase Matching Bandwidth Experiments

3. Theoretical Comparison of Phase Matching Bandwidth

Appendix B: Coupled-Wave Equations

Here we derive the coupled wave equations that describe coherent stimulated Brillouin scattering involving a pump, Stokes, probe, and backscattered optical field given respectively by

$$\tilde{E}_P(z,t) = A_P e^{i(k_P z - \omega_P t)} + c.c. \tag{B1}$$

$$\tilde{E}_S(z,t) = A_S e^{i(k_S z - \omega_S t)} + c.c. \tag{B2}$$

$$\tilde{E}_{Pr}(z,t) = A_{Pr} e^{i(k_{Pr} z - \omega_{Pr} t)} + c.c. \tag{B3}$$

$$\tilde{E}_{Sig}(z,t) = A_{Sig} e^{i(k_{Sig} z - \omega_{Sig} t)} + c.c. \tag{B4}$$

and a common acoustic field given by

$$\tilde{\rho}(z,t) = \rho_0 + \rho(z,t) e^{i(qz - \Omega t)} + c.c., \tag{B5}$$

where $\Omega = \omega_P - \omega_S$ and $q = k_P - k_S = 2k_P$.

1. Acoustic Field

As in the case of SBS [2], we start by assuming that the material obeys the acoustic wave equation,

$$\frac{\partial^2\tilde{\rho}}{\partial t^2} - \Gamma'\nabla^2\frac{\partial\tilde{\rho}}{\partial t} - v^2\nabla^2\tilde{\rho} = \nabla\cdot\vec{f}, \tag{B6}$$

where v is the sound speed in the material and Γ' is a damping parameter given by

$$\Gamma' = \frac{1}{\rho}\left[\frac{4}{3}\eta_s + \eta_b + \frac{\kappa}{C_p}(\gamma-1)\right], \tag{B7}$$

where η_s and η_b are the shear and bulk viscosity coefficients of the material, respectively. The source term on the right side of Eq. (B6) is the divergence of the electrostrictive force:

$$\vec{f} = \nabla p_{st} = \nabla\cdot\left[-\frac{1}{2}\epsilon_0\gamma_e\Big(\langle\tilde{E}_P\cdot\tilde{E}_S\rangle + \langle\tilde{E}_{Pr}\cdot\tilde{E}_{Sig}\rangle\Big)\right], \tag{B8}$$

which yields, after applying the slowly varying amplitude approximation,

$$\nabla\cdot\vec{f} = \epsilon_0\gamma_e q^2(A_P A_S^* + A_{Pr}A_{Sig}^* e^{i\Delta kz}), \tag{B9}$$

Where $\Delta k = (k_{Pr} - k_{Sig}) - (k_P - k_S)$ is the phase mismatch between the four optical fields. Only two electrostrictive terms survive terms after accounting for the orthogonal polarization of the pump and Stokes fields with respect to that of the probe and backscattered signal. Inserting this electrostrictive force term and the acoustic field (Eq. (B5)) into Eq. (B6) and assuming a slowly varying acoustic amplitude we find

$$-2i\Omega\frac{\partial\rho}{\partial t} - \Gamma' 2iq^2\Omega\rho - 2iqv^2\frac{\partial\rho}{\partial z} = \epsilon_0\gamma_e q^2(A_P A_S^* + A_{Pr}A_{Sig}^* e^{i\Delta kz}), \tag{B10}$$

which can be restated in terms of the Brillouin linewidth, $\Gamma_B = q^2\Gamma'$, as

$$-2i\Omega\frac{\partial\rho}{\partial t} - 2i\Omega\Gamma_B\rho - 2iqv^2\frac{\partial\rho}{\partial z} = \epsilon_0\gamma_e q^2(A_P A_S^* + A_{Pr}A_{Sig}^* e^{i\Delta kz}). \tag{B11}$$

Given the phonon dispersion relations $\Omega_B = |q_B|v$ and $\Omega^2 = q^2\left(v^2 - i\Omega\Gamma'\right)$, Eq. (B11) can be rewritten as

$$-2i\Omega\frac{\partial\rho}{\partial t} + \left(\Omega^2 - \Omega^2 - i\Omega\Gamma_B\right)\rho - 2iqv^2\frac{\partial\rho}{\partial z} = \epsilon_0\gamma_e q^2(A_P A_S^* + A_{Pr}A_{Sig}^* e^{i\Delta kz}). \tag{B12}$$

We take the common assumption that the phonon propagation distance is small compared to the distance over which the source term varies significantly, which allows the spatial derivative term in Eq. (B12). We further assume steady-state conditions such that the time derivative term also vanishes, leaving

$$(\Omega_B^2 - \Omega^2 - i\Omega\Gamma_B)_\rho = \epsilon_0\gamma_e q^2(A_P A_S^* + A_{Pr}A_{Sig}^* e^{i\Delta kz}). \tag{B13}$$

We thus find the acoustic field amplitude to be

$$\rho(z,t) = \epsilon_0\gamma_e q^2\frac{A_P A_S^* + A_{Pr}A_{Sig}^* e^{i\Delta kz}}{\Omega_B^2 - \Omega^2 - i\Omega\Gamma_B}. \tag{B14}$$

2. Optical Fields

We now turn to the spatial evolution of the optical fields, described by the wave equation,

$$\frac{\partial^2 \tilde{E}_i}{\partial z^2} - \frac{n^2}{c^2}\frac{\partial^2 \tilde{E}_i}{\partial t^2} = \frac{1}{\epsilon_0 c^2}\frac{\partial^2 \tilde{P}_i}{\partial t^2}, \tag{B15}$$

where i denotes the four optical fields, namely: pump, Stokes, probe, and backscattered signal. The total nonlinear polarization that gives rise to the source term in the wave equation is given by

$$\tilde{P} = \epsilon_0 \Delta\chi \tilde{E} = \epsilon_0 \Delta\epsilon \tilde{E} = \epsilon_0 \rho^{-1} \gamma_e \tilde{\rho} \tilde{E}. \tag{B16}$$

The parts of $\tilde{P}$ that can act as phase-matched source terms for the optical fields are

$$\tilde{P}_P = p_P e^{i(k_P z - \omega_P t)} + c.c. = \frac{1}{2}\epsilon_0 \rho_0^{-1} \gamma_e \rho A_S e^{i(k_P z - \omega_P t)} \tag{B17}$$

$$\tilde{P}_S = p_S e^{i(-k_S z - \omega_S t)} + c.c. = \frac{1}{2}\epsilon_0 \rho_0^{-1} \gamma_e \rho^* A_P e^{i(-k_S z - \omega_S t)} \tag{B18}$$

$$\tilde{P}_{Pr} = p_{Pr} e^{i(k_{Pr} z - \omega_{Pr} t)} + c.c. = \frac{1}{2}\epsilon_0 \rho_0^{-1} \gamma_e \rho A_{Sig} e^{i(k_{Pr} z - \omega_{Pr} t)} e^{i\Delta k z} \tag{B19}$$

$$\tilde{P}_{Sig} = p_{Sig} e^{i(-k_{Sig} z - \omega_{Sig} t)} + c.c. = \frac{1}{2}\epsilon_0 \rho_0^{-1} \gamma_e \rho^* A_{Pr} e^{i(-k_{Sig} z - \omega_{Sig} t)} e^{-i\Delta k z}. \tag{B20}$$

Inserting the optical fields (Eqs. B1-B4) and phase-matched source terms (Eqs. B17-B20) into Eq. (B15), we obtain

$$\frac{\partial A_P}{\partial z} + \frac{n}{c}\frac{\partial A_P}{\partial t} = \frac{i\omega_P \gamma_e}{2nc\rho_0}\rho A_2 \tag{B21}$$

$$-\frac{\partial A_S}{\partial z} + \frac{n}{c}\frac{\partial A_S}{\partial t} = \frac{i\omega_S \gamma_e}{2nc\rho_0}\rho^* A_P \tag{B22}$$

$$\frac{\partial A_{Pr}}{\partial z} + \frac{n}{c}\frac{\partial A_{Pr}}{\partial t} = \frac{i\omega_{Pr} \gamma_e}{2nc\rho_0}\rho A_{Sig} \tag{B23}$$

$$-\frac{\partial A_{Sig}}{\partial z} + \frac{n}{c}\frac{\partial A_{Sig}}{\partial t} = \frac{i\omega_{Sig} \gamma_e}{2nc\rho_0}\rho^* A_{Pr} \tag{B24}$$

We again assume steady-state conditions, allowing the time derivative term to be dropped. Plugging in the acoustic

field amplitude (Eq. B14), we arrive at the coupled-amplitude wave equations for the optical fields,

$$\frac{\partial A_P}{\partial z} = \frac{i\epsilon_0\omega_P q^2\gamma_e^2}{2nc\rho_0}\frac{A_P|A_S|^2 + A_{Pr}A_{Sig}^* A_S e^{i\Delta kz}}{\Omega_B^2 - \Omega^2 - i\Omega\Gamma_B} \tag{B25}$$

$$\frac{\partial A_S}{\partial z} = -\frac{i\epsilon_0\omega_S q^2\gamma_e^2}{2nc\rho_0}\frac{|A_P|^2 A_S^* + A_{Pr}A_{Sig}^* A_P e^{-i\Delta kz}}{\Omega_B^2 - \Omega^2 - i\Omega\Gamma_B} \tag{B26}$$

$$\frac{\partial A_{Pr}}{\partial z} = \frac{i\epsilon_0\omega_{Pr} q^2\gamma_e^2}{2nc\rho_0}\frac{A_P A_S^* A_{Sig} + A_{Pr}|A_{Sig}|^2 e^{i\Delta kz}}{\Omega_B^2 - \Omega^2 - i\Omega\Gamma_B} \tag{B27}$$

$$\frac{\partial A_{Sig}}{\partial z} = -\frac{i\epsilon_0\omega_{Sig} q^2\gamma_e^2}{2nc\rho_0}\frac{A_P A_S^* A_{Pr} + |A_{Pr}|^2 A_{Sig}^* e^{-i\Delta kz}}{\Omega_B^2 - \Omega^2 - i\Omega\Gamma_B} \tag{B28}$$

Integrating Eq. B28 along the effective length gives the amplitudes of each optical field,

$$A_P = \frac{i\epsilon_0\omega_P q^2\gamma_e^2}{2nc\rho_0}\frac{A_P|A_S|^2 + A_{Pr}A_{Sig}^* A_S}{\Omega_B^2 - \Omega^2 - i\Omega\Gamma_B}\frac{e^{i\Delta kL} - 1}{i\Delta k}, \tag{B29}$$

$$A_S = -\frac{i\epsilon_0\omega_S q^2\gamma_e^2}{2nc\rho_0}\frac{|A_P|^2 A_S^* + A_{Pr}A_{Sig}^* A_P}{\Omega_B^2 - \Omega^2 - i\Omega\Gamma_B}\frac{e^{-i\Delta kL} - 1}{-i\Delta k}, \tag{B30}$$

$$A_{Pr} = \frac{i\epsilon_0\omega_{Pr} q^2\gamma_e^2}{2nc\rho_0}\frac{A_P A_S^* A_{Sig} + A_{Pr}|A_{Sig}|^2}{\Omega_B^2 - \Omega^2 - i\Omega\Gamma_B}\frac{e^{i\Delta kL} - 1}{i\Delta k}, \tag{B31}$$

$$A_{Sig} = -\frac{i\epsilon_0\omega_{Sig} q^2\gamma_e^2}{2nc\rho_0}\frac{A_P A_S^* A_{Pr} + |A_{Pr}|^2 A_{Sig}^*}{\Omega_B^2 - \Omega^2 - i\Omega\Gamma_B}\frac{e^{-i\Delta kL} - 1}{-i\Delta k}. \tag{B32}$$

The intensity of the backscattered signal is given by the magnitude of the time-averaged Poynting vector, given by

$$I_i = 2n_i\epsilon_0 c|A_i|^2, \qquad i = 1, 2, 3, \tag{B33}$$

which gives

$$I_{Sig} = \frac{\epsilon_0^2\omega^2 q^4\gamma_e^4}{4n^2c^2\rho_0^2}\frac{|A_P|^2|A_S|^2|A_{Pr}|^2}{(\Omega_B - \Omega)^4 - \Omega^2\Gamma_B^2}\left|\frac{e^{-i\Delta kL} - 1}{-i\Delta k}\right|^2. \tag{B34}$$

Here we have taken the real part and dropped the very small terms containing the signal amplitude. The squared

modulus term containing Δk can be reduced as

$$\left|\frac{e^{-i\Delta kL}-1}{-i\Delta k}\right|^2 = \frac{(e^{-i\Delta kL}-1)(e^{i\Delta kL}-1)}{(\Delta k)^2} = \frac{L^2}{(\Delta kL)^2}\left[2-2\left(\frac{e^{i\Delta kL}+e^{-1\Delta kL}}{2}\right)\right]$$

$$= \frac{2L^2(1-cos\Delta kL)}{(\Delta kL)^2} = \frac{4L^2 sin^2\left(\frac{\Delta kL}{2}\right)}{\left(\Delta kL\right)^2} = \frac{L^2 sin^2\left(\frac{\Delta kL}{2}\right)}{\left(\frac{\Delta kL}{2}\right)^2} = L^2 sinc^2\left(\frac{\Delta kL}{2}\right) \tag{B35}$$

and the optical fields can be written in terms of the intensities to produce the backscattered intensity of the signal:

$$I_{Sig} = \frac{\epsilon_0^2\omega^2 q^4\gamma_e^4}{4n^2c^2\rho_0^2}\frac{I_P I_S I_{Pr}}{(\Omega_B-\Omega)^4-\Omega^2\Gamma_B^2}L^2 sinc^2\left(\frac{\Delta kL}{2}\right). \tag{B36}$$

Defining the intensities as $I_i = 2n\epsilon_0 cA_i A_i^*$, the backscattered signal intensity is reduced to [see green writing to far right in onenote coupled wave equations of CABS]

To find the power of the backscattered signal, we would integrate this intensity over the effective area. Approximated for fiber as πr^2 where r is the effective mode field diameter, this becomes

$$P_{Sig} = \pi r^2\frac{\epsilon_0^2\omega^2 q^4\gamma_e^4}{4n^2c^2\rho_0^2}\frac{P_P P_S P_{Pr}}{(\Omega_B-\Omega)^4-\Omega^2\Gamma_B^2}L^2 sinc^2\left(\frac{\Delta kL}{2}\right). \tag{B37}$$

[1] P. Maker, R. Terhune, M. Nisenoff, and C. Savage, Effects of dispersion and focusing on the production of optical harmonics, Physical review letters **8**, 21 (1962).
[2] R. W. Boyd, *Nonlinear Optics* (Academic Press, 2020).